A Hybrid Chaotic MPA-PID Controller for Voltage Profile Enhancement in Solid State Transformer-Connected Pantograph System for Charging an Electric Bus

Dinakar Yeddu*, B. Loveswara Rao**‡

*Research Scholar, Department of Electrical and Electronics Engineering , Koneru Lakshmaiah Education Foundation, Vaddeswaram, AP,India .

**Professor, Department of Electrical and Electronics Engineering, Koneru Lakshmaiah Education Foundation, Vaddeswaram AP, India.

(2002060001@kluniversity.in,loveswararao@kluniversity.in)

‡Corresponding Author; B.Loveswara Rao, Department of Electrical and Electronics Engineering,

Koneru Lakshmaiah Education Foundation, Vaddeswaram,AP,India

Tel: +91 9866290922, loveswararao@kluniversity.in

Received: 18.03.2023 Accepted:11.04.2023

Abstract- The article proposes a novel design of DC pantograph system charging of electric buses using a solid-state transformer and also proposes an efficient Marine predator's algorithm optimizer with a novel chaotic behaviour to optimize the gains in the PID controller of the DC-DC forward converter voltage control. The Ch-MPA is based on a circle map of chaotic type to increase convergence and achieve global minima. The results are compared with other algorithms, like WOAPID and SAPID controllers .Transient response analysis ,frequency response (Bode) analysis ,and performance indices analysis were carried out on the MATLAB/Simulink platform. The simulation results of the proposed approaches are effective, and Ch-MPAPID and MPAPID for the DC-DC forward converter voltage control demonstrated superior performance.

Keywords Solid State Transformer, Pantograph System, Electric Bus, DC-DC Forward Converter Voltage Control, PID, Chaotic Marine Predators Algorithm Optimizer, Transient Response.

1. Introduction

Environmental pollution (CO_2,NOx and CO) is caused by automobiles ,which use fossil fuels. This is further contributing to warming and air quality [1]-[3].The humans inhaling of air causes defects in their organs [4]-[6].Electric Vehicles(EVs) are gaining increased attention as a result of environmental problems like carbon emissions and the depletion of natural resources .The expensive batteries and issues with performance deterioration must be fixed for EVs to be practical and widely used.

Conditions of use have a significant impact on how the battery degrades in terms of energy capacity and power capabilities[7]. However ,when there are more electric vehicles on the road ,the distribution network will have high energy demand[8].Increasing the number of electric vehicles(EVs) in residential parking lots has recently become a significant problem since too many EVs can cause the power grid to become unstable when there is a large demand for charging[9].One study recommends building out the continuous infrastructure to prevent the grid consequences of large-scale EV charging ,loads would produce unaffordable prices[10].

Transit agencies in developed countries are making significant investments in the electrification of vehicles to fight the growing health difficulties and environmental worries about greenhouse gases, combustion smells ,and energy efficiency[11].

The solid-state transformer with a medium-frequency link originated due to the development of semiconductor technology and integrating distribution generation into LV ac or dc grids[12].SST can do a variety of grid integration activities, such as replacement of LFT in conventional grids[13],the interface between the MV grid and the smart grid, which have distribution generation and control features[14].

SST also have applications in traction[15].Since microgrids have a high ability to nurture and enhance the integration of renewable energy sources, the idea of using them in the distribution of electrical energy has gained a lot of interest. They also enable increased system efficiency and power quality[16].

The proportional-integral-derivative (PID) controller is the most often used one in the business world, but it only works well when its settings are adjusted precisely .Although conventional techniques like pole placement and Ziegler's -Nicholas have been employed in the past for this job ,the use of cutting-edge techniques like heuristic optimization algorithms has grown in popularity recently[17-19].

The bacterial foraging algorithm(BFA)[20],the firefly algorithm(FA) [21],the (PSO)[22],the (GA)[23],and the WOA[24].All these techniques applied for DC-DC buck converter voltage control, fine tuning PID controller parameters that have been researched in the Literature.

The heuristics algorithm searches a large space randomly and reaches the optimum or is near the optimum .Convergence depends on the random numbers generated by the algorithm run[25].To achieve better results chaotic sequences were used in place of random numbers .This is leading to a new trend in heuristics opt that aim to achieve better results[26].In [27] the Chebyshev ,circle ,Gauss /mouse, iterative ,logistic ,piece-wise, sine, singer, sinusoidal ,and tent maps are among the 10 chaotic maps .

This article presents the Marine Predators Algorithm (MPA).Previously it dealt with mathematical test functions and engineering design problems in areas of ventilation and building energy performance, not in power converters application. It uses levy or Brownian movement, when food is sparse, use levy movement or else Brownian .It is a high-performance optimizer[28].

The paper is structured as follows :section 2 discusses a novel design of SST-based DC pantograph system, is proposed, simulated, and shown results,section3 discusses the proposed novel hybrid algorithm 'circle' chaotic (ChMPA-PID).Section 4 discusses the forward converter model and PID controller .Section 5 and 6 simulation results were presented.

2. Proposed Design of SST Based Pantograph System for Charging of EB.

2.1. SST Topology

Over the past 20 years, solid state transformer technology has improved quickly .As a result, low frequency transformers are currently being replaced by solid state transformers in traction applications ,which results in significant weight and volume reductions and reliability increases.[29].The standard transformer can be replaced with the SST to charge the electric bus. The block diagram for the solid-state transformer is displayed in Figure 1 below.

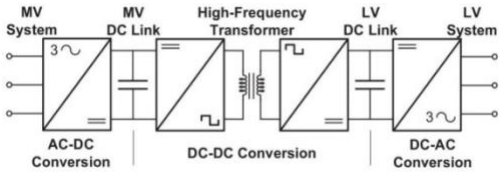

Fig. 1. SST's block diagram[30].

The SST architecture features a feature that allows power to be supplied to DC loads. The conversion stages used in the SST configuration have an overall efficiency of 94% is anticipated [31].([AC-DC ,DC-DC,DC-AC]).

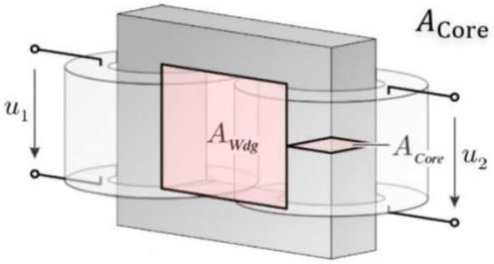

Fig.2.TF core[32].

$$\text{Area Product: Acore. Awdg} = \sqrt{2}/\pi \ \frac{P_t}{K_w J_{rms} B_{max} f}$$

$$\text{Volume: } V \propto \left(A_{core} A_{wdg}\right)^{3/4} \propto \frac{1}{(f)^{3/4}} \quad (1)$$

It is possible to reduce a transformer's volume and weight while keeping its overall core flux density (B_{MAXT})and winding current density (J_{RMS}),as shown by the area product. The power to be transmitted is shown in Eq.(1).The transformer design equation is shown in Eq.(2).

$$V_{pri} = \sqrt{2}\,.\,\pi.\,f.\,N_{pri}.\,\phi_m = 4.44.\,f.\,N_{pri} B_m.\,A \quad (2)$$

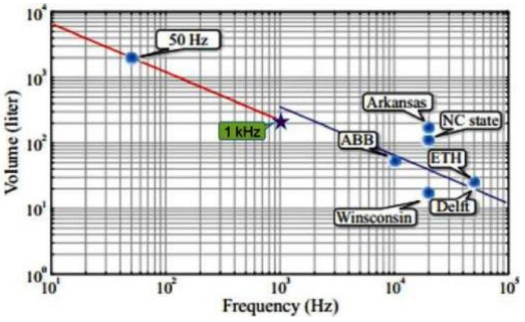

Fig. 3. Transformer Volume vs Frequency[33].

The higher power transmission efficiency of SSTs would be particularly advantageous for systems with volume and weight constraints .Future differentiation is more controllable with MF transformers than with other discrete

power electronic converters that link to MV via a low-voltage (LV) input. An SST regulates line and load disturbances .In Figure3 ,the blue line uses a silicon steel core ,while the red line uses a ferrite core. The silicon core material is suitable for frequencies between 1 and 1.5KHZ.

2.2. 1-MVA ,11KV-AC/415V-AC and 800V-DC Solid-State Transformer

Transformers provide galvanic isolation and voltage scaling for today's power networks .Although these components work and are dependable ,their passive architecture severely restricts the options for control .Regional low-voltage AC or DC delivery systems or microgrids ,are linked to medium voltage grids via SSTs, which are power electronic networks .

Reactive power adjustment ,active harmonic filtering ,peak load sharing and other characteristics are made possible by the high degree of controllability, stability, and galvanic isolation that SSTs possess.

Here, taking into account the bidirectional distribution - level SST systems efficiency and power density ,one fully rated 80KW converter cell has been achieved.

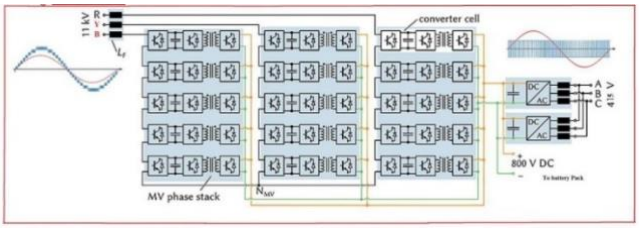

Fig. 4. schematic diagram of solid-state transformer[34].

2.3. CASE-1: If the Input is AC Then the Mathematical Modelling is as Follows.

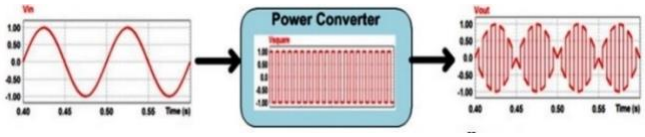

$$V_{in} = \sqrt{2}\, V_{in.rms}.\sin(\omega_s \,.\, t) \quad * \quad S_{square} = \frac{4}{\pi}.\sum_{n=1,3,5}^{\infty} \frac{1}{n} cos(n.\,\omega_{sq}\,.\,t)$$

$$V_{out}=V_{in.rms}\begin{bmatrix} 0.9.sin(\omega_{sq} \pm \omega_s).\mathrm{t}) \\ +\,0.23.sin(3\omega_{sq} \pm \omega_s).\mathrm{t}) \\ +0.15.sin(5\omega_{sq} \pm \omega_s).\mathrm{t}) \\ +\,high\ order\ terms \end{bmatrix}$$

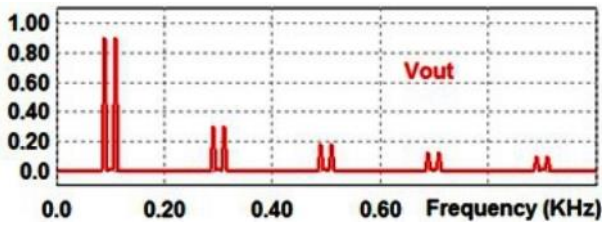

Fig. 5. square wave switching fucntion for AC input.

With the help of the switching function ,we get high-frequency AC from low-frequency AC input .The output voltage's frequency spectrum (FFT) ,which is depicted in Fig.5 supports the equations.

2.4. CASE-2: If the Input is DC When we use Solar Integration in that Case we go for Mathematical Modelling

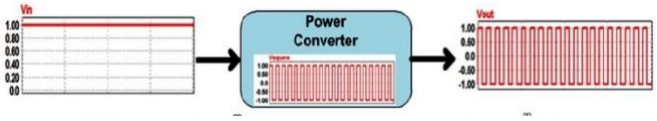

$$V_{in} = V_{dc} \quad * \quad S_{square} = \frac{4}{\pi}.\sum_{n=1,3,5}^{\infty} \frac{1}{n} sin(n.\,\omega_{sq}\,.\,t)$$

$$= \quad V_{out} = \frac{4}{\pi}.V_{dc}\sum_{n=1,3,5}^{\infty} \frac{1}{n} sin(n.\,\omega_{sq}\,.\,t)$$

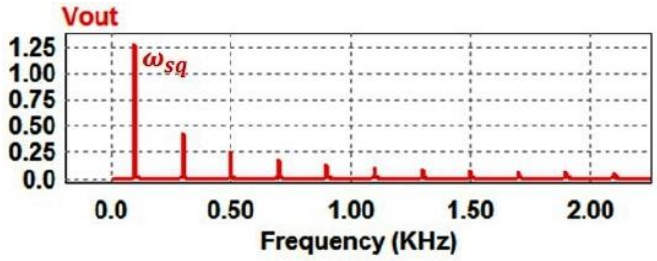

Fig. 6. square wave switching function for DC input.

When a high frequency square wave is the intended output and the input is a DC signal ,in Fig.6,a power converter switching function is shown. The output voltage's frequency spectrum (FFT) ,which is depicted in Fig.6 ,supports the equations.

2.5. Pantograph System

Using pantograph technology, electric vehicles may be charged quickly at bus stops. It has DC charging hardware. On the top of the vehicle are installed communications systems ,positive and negative poles ,automatic connections from the top, and established conductive paths .This subject has a specific research focus. A connection device linked to the infrastructure above the vehicle for conductive charging is monitored and managed by the automatic connecting system. The voltage range of a DC EV conductive charging system is 450-750V and it can generate 450KW of electricity. ABB provides the well-known pantograph system, OPP-Charge Fig.7[35]. Shows a pantograph apparatus in action.

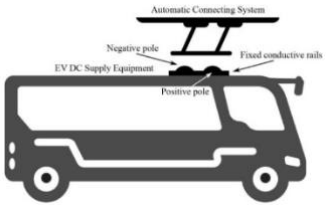

Fig. 7. DC Pantograph system.

The novel pantograph charging system with solid state transformer-based 11KV/1MVA/800V was simulated[36] as shown in Fig.8 and output voltage is 800V DC. They are currently getting ready to charge the electric bus. The output voltage waveform is seen in Fig.9.The parameters of SST are displayed in table 1 for simulation purposes.

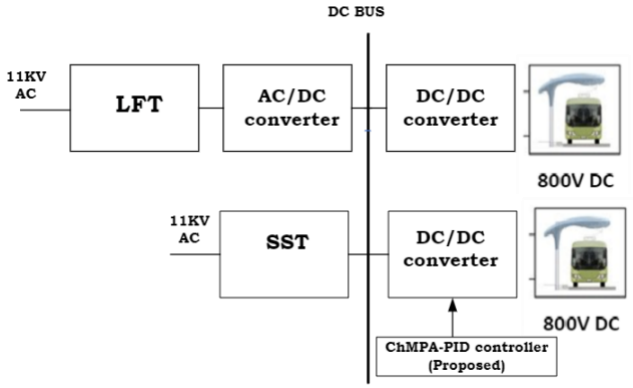

Fig. 8. Conventional ,proposed SST based Pantograph charging system block diagram.

Table 1. Parameters of SST

Parameters	**Values**
Input, V_i	11KV-AC
Output, V_o	DC-800V
C_{MV}	500nF
C_{LV}	70 μF
TR mag ind (L_h)	4.1mH
TR lea ind ($L\sigma$)	195μH
Fsw	50khz

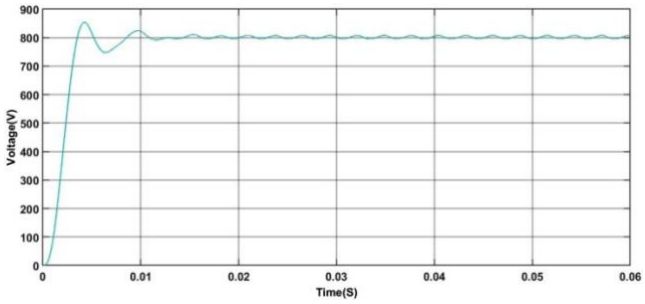

Fig. 9. SST output voltage waveform.

3. The proposed Heuristic optimization algorithm

3.1. Marine Predators Algorithm

A nature inspired optimization method ,MPA that mimics how predators and prey in marine environments select their ideal foraging tactics and how frequently they come into contact. Depending on the quantity of prey ,sharks ,tuna and other fish use Brownian motion or levy motion.[37].It also takes into account the relative speeds of the predator and prey[38].MPA formulation and the initial solution are given by Eq.(3).

$$X_0 = X_{min} + rand(X_{max} - X_{min}) \quad (3)$$

X_{min} and X_{max} are the LB and UB for variables and rand[0,1]

$$ELITE = \begin{bmatrix} X^I_{1,1} & X^I_{1,2} & \dots & X^I_{1,d} \\ X^I_{2,1} & X^I_{2,2} & \dots & X^I_{2,d} \\ . & . & . & . \\ . & . & . & . \\ X^I_{n,1} & X^I_{n,2} & \dots & X^I_{n.d} \end{bmatrix} nxd \quad (4)$$

Apex predators in nature are better foragers as per the notion of survival of the fittest theory.As a result ,the top predator in the Elite matrix is chosen as the fittest solution.The top predator vector is represented by the arrays of this matrix ,which oversee searching for and finding the prey based on information about the placements of the prey ,in which $\overrightarrow{X^t}$ is top predator vector.

There are n search agents and d dimensions respectively.It should be remembered that search agents include both predators and their victims.Because the prey is already searching for its own sustenance by the time the predator is seeking for its prey .Following each repetition,if a better predator replaces the top predator,the elite will be updated.

Prey is a different matrix with the same dimension as Elite,and predators adjust their positions in response to it.To put it simply,initialization produces the initial prey ,from which the fittest individual (predator) builds the Elite.As shown ,the prey is as follows.

$$Prey = \begin{bmatrix} X_{1,1} & X_{1,2} & \dots & X_{1,d} \\ X_{2,1} & X_{2,2} & \dots & X_{2,d} \\ X_{3,1} & X_{3,2} & \dots & X_{3,d} \\ . & . & . & . \\ . & . & . & . \\ X_{n,1} & X_{n,2} & \dots & X_{n,d} \end{bmatrix} nxd \quad (5)$$

The MPA optimization method is broken down into three primary steps that take into account various velocity ratios while also simulating the complete lives of a predator andprey:(1)V_{prey}>$V_{predator}$.(2)V_{prey}=$V_{predator}$.(3)$V_{predator}$> V_{prey}.

A precise duration of iteration is designated and assigned for each phase that is determined.These procedures are specified based on the laws predator and prey movements are modelled after those found in nature and are managed accordingly.The three steps include.

Phase1: While iter $< \frac{1}{3}$ Max_iter

$$\overrightarrow{stepsize_i} = \overrightarrow{R_B} \otimes (\overrightarrow{Elite_i} - \overrightarrow{R_B} \otimes \overrightarrow{prey_i}) \quad i=1,..n$$
$$\overrightarrow{prey_i} = \overrightarrow{prey_i} + P.\vec{R} \otimes \overrightarrow{Stepsize_i} \quad (6)$$

Phase2: While $\frac{1}{3}$ Max_iter $<$ Iter $< \frac{2}{3}$ Max_iter

For the first half of the population.

$$\overrightarrow{stepsize_i} = \overrightarrow{R_L} \otimes (\overrightarrow{Elite_i} - \overrightarrow{R_L} \otimes \overrightarrow{prey_i}) \quad i=1...n/2$$

$$\overrightarrow{prey_i} = \overrightarrow{prey_i} + P.\vec{R} \otimes \overrightarrow{Stepsize_i} \quad (7)$$

For the second half of the population.

$$\overrightarrow{stepsize_i} = \overrightarrow{R_B} \otimes (\overrightarrow{R_B} \otimes \overrightarrow{Elite_i} - \overrightarrow{prey_i}) \quad i=n/2,..n$$

$$\overrightarrow{prey_i} = \overrightarrow{Elite_i} + P.CF \otimes \overrightarrow{Stepsize_i} \quad (8)$$

Phase3:While iter $> \frac{2}{3}$ Max_iter

$$\overrightarrow{stepsize_i} = \overrightarrow{R_L} \otimes (\overrightarrow{R_L} \otimes \overrightarrow{Elite_i} - \overrightarrow{prey_i}) \quad i=1..n$$

$$\overrightarrow{prey_i} = \overrightarrow{Elite_i} + P.CF \otimes \overrightarrow{Stepsize_i} \quad (9)$$

Eddy and FAD's effect

$$\overrightarrow{Prey_i} = \begin{cases} \overrightarrow{Prey_i} + CF[\vec{X}_{min} + \vec{R} \otimes (\vec{X}_{max} - \vec{X}_{min})] \otimes \vec{U} & if\ r \le FADs \\ \overrightarrow{Prey_i} + [FADs(1-r) + r](\overrightarrow{Prey_{r1}} - \overrightarrow{Prey_{r2}}) & if\ r > FADs \end{cases} \quad (10)$$

3.1.1 Marine Memory

Based on the aspects that have been highlighted ,it can be concluded that marine predators have good memory .Memory saving in MPA simulates this capability .This matrix is assessed for fitness to update the Elite after the prey has been updated and the FADs impact has been applied.Every solution in the current iteration is compared to its equivalent in the previous iteration for fitness ,and if the current one is more suited ,it replaces the previous one .This method replicates predators returning to the locations of the prey-abundant area after succesful foraging and also enhances the quality of the solution with each iteration (Parouha & Das,2016).The MPA pseudo-code is given in Algorithm-1 .

Algorithm 1: Pseudocode of MP Algorithm

Initialize search agents (prey) populations i=1,....n
While termination criteria are not met
Calculate the fitness and construct the Elite matrix
İf Iter<Max_Iter/3
Update prey based on Eq.6
Else if Max_iter/3<Iter<2*Max_Iter/3
For the first half of the populations(i=1,....,n/2)
Update prey based on Eq.7
For the other half of the populations(i=n/2,...,n)
Update prey based on Eq.8
Else if Iter>2*Max_Iter/3
Update prey based on Eq.9
End(if)
Accomplish memory saving and Elite update
Applying FADs effect and update based on Eq.10
End **while**

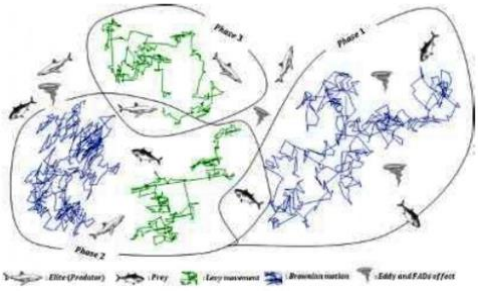

Fig. 10. showing phases of MPA algorithm[39].

3.2. The Novel Chaotic Marine Predator's Algorithm (ChMPA)

Several metaheuristic algorithms in use today use randomness or specific parameters that must be adjusted. However ,choosing the parameters could be difficult because they might vary depending on the dataset .So, harnessing chaos to solve the aforementioned issue can be successful. Randomness ,non-repetition, ergodicity ,and the ability for the initial condition to change nonlinearity for future behaviour are all characteristics of chaos .There are 12 distinct chaotic maps .This uses the circle chaotic map equation ,which is presented in Eq.(11)[40].

$$x_{k+1} = \mathrm{mod}(x_k + \beta - (\frac{\alpha}{2\pi})\sin(2\pi x_k),1) \quad (11)$$

$$\alpha = 0.5\,;\beta = 0.2$$

The visualization of the circle chaotic map is shown in Fig.11

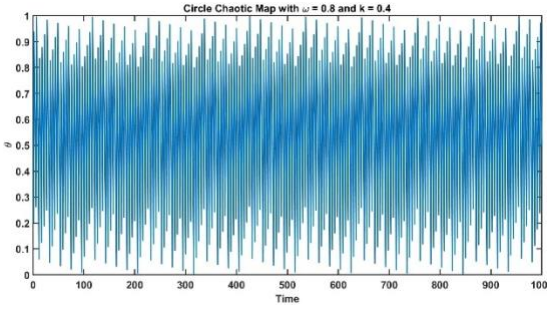

Fig. 11. visualization of circle chaotic map.

The combination of MPA and the chaotic map gives the proposed ChMPA .In this updation shown below ,update the levy exponent using circle chaotic map in code.

beta=mod(a * beta +b,1) (12)

4. DC-DC Forward Buck Converter Model

4.1. Forward Buck Converter Open Loop Step Response

The equivalent circuit of the DC-DC converter is considered for voltage control and is shown in Fig.12.The open loop transfer function model is represented as below .Here ,in continuous conduction mode ,the voltage across the resistor is given by Eq.13.

Table 2. Parameters of DC-DC forward converter.

Parameters	Values
V_{in}	$36V_{DC}$
V_{ref}	$12V_{DC}$
N2:N1	1:1
R_L	6 Ω
L	1_{mH}
C	100 µF
D	1/3
F_{sw}	40KHZ

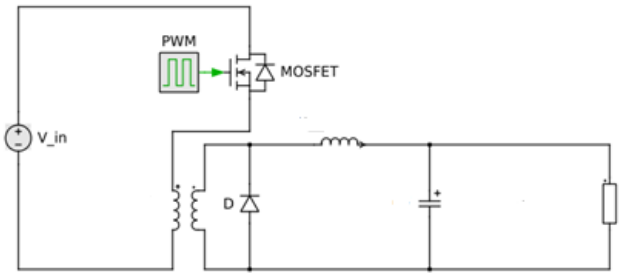

Fig. 12. Forward Buck Converter

$$V_{out} = \frac{N_2}{N_1} * D * V_{in} \quad (13)$$

In this turns ratio is taken as 1.Then OLTF is

$$OLTF(s) = \frac{\frac{V_i}{LC}}{S^2+\frac{1}{RC}S+\frac{1}{LC}} \quad (14)$$

For the purpose of analysis in simulation of step response ,reference voltage is taken as less & resistance is taken as load.Table 2 shows parameters and values.

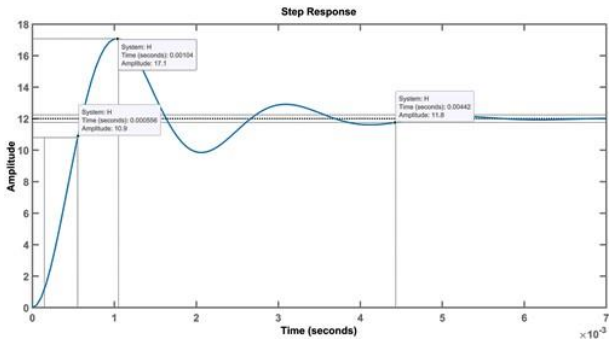

Fig. 13. Forward Buck converter open loop step response.

In the absence of the controller the transient response needs İmprovement

Table 3. Ch-MPA algorithm parameters

Parameters	Values
Number of Population	25
Maximum iteration no	30
Lower bounds for (kp,ki, kd,)	[1 0.01 0.001]
Upper bounds	[50 10 0.01]
a; b	0.5;0.2

4.2. DC-DC Forward Buck Converter Voltage Control with PID Controller.

The closed loop control of a DC-DC converter with a PID controller ,Fig.14 depicts the block diagram of it. To get the optimal step response ,we need to tune the gains of the controller. The closed loop transfer function with unity feedback is given as

$$CLTF(s)=\frac{\frac{V^2}{LC}(s.K_p+K_i+s^2K_d}{s^3+s^2[\frac{1}{RC}+\frac{V_iK_d}{LC}]+s[\frac{1}{LC}+\frac{K_pV_i}{LC}]+K_i} \quad (15)$$

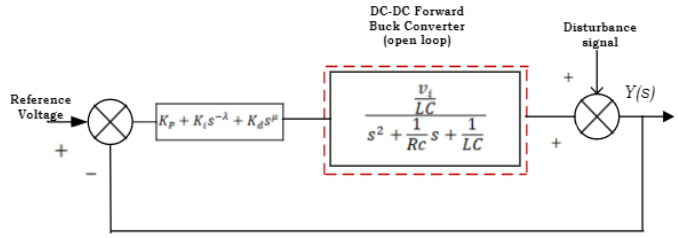

Fig. 14. Forward Buck converter with PID controller, block diagram.

5. Simulation results and discussions

5.1. Implementation of the Proposed Ch-MPA-PID Approach for DC-DC Forward Buck Converter.

The objective function ITAE is used for comparison for different algorithms .The e(t) is the error between the output and reference voltage .Tsim is $3*10^{-6}$.To compare fairly with[24],the same ITAE is adopted, and its mathematical representation is shown in Eq.(16).

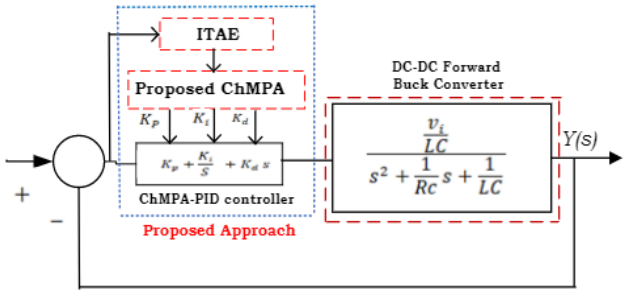

Fig. 15. Proposed Ch-MPA-PID controller approach in DC-DC forward buck converter voltage control block diagram.

Table. 4. optimal gains of PID using algorithms

Algorithm controller	Kp	Ki	Kd
Ch MPA PID (proposed)	1.7865	8.4914	0.0187
MPA PID (proposed)	2.7499	8.4928	0.0094
WOAPID[24]	43.5764	7.85992	0.008994
SA PID[24]	40.3741	9.45461	0.007808

Using the proposed algorithm ,the optimal values are found, and it has excellent searching strategies. Table 4 shows the various algorithms optimal values listed .Fig.15 depicts the block diagram of the proposed approach.

With the completion of optimization ,the optimal gains are used for deriving the CLTF and analysis will be made from here onwards .The flow chart of the proposed ChMPA-PID is shown in Fig.16.,when the max iterations

,as per table 3 reached the program stops and gives the optimal values.

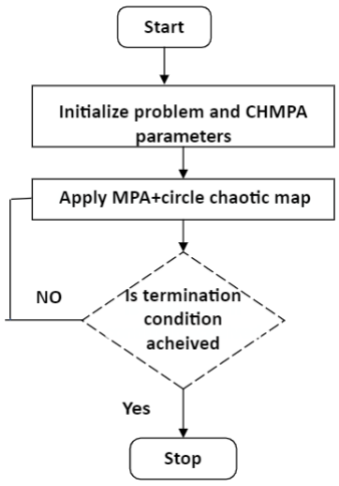

Fig. 16. Flowchart of ChMPA

.

5.2 Transient response analysis

The criteria of transient response of all algorithms are shown in table 5 and Fig.17.Among all Ch-MPA,MPA (proposed) have performed well and shown the improved transient response and bar chart is depicted in Fig.18

Table 5. Parameters of Transient Response

Algorithm controller	Over shoot (%)	Settling time(s) (+-2%)	Rise time(s) (0.10-0.90)
Ch-MPAPID (proposed)	0	$0.558271x10^{-6}$	$3.2659x10^{-6}$
MPA PID (proposed)	0	$1.1618x10^{-6}$	$6.5019 x10^{-6}$
WOAPID[24]	0	$1.1950 x10^{-6}$	$6.7658x10^{-6}$
SAPID [24]	0	$1.3726 x10^{-6}$	$7.7874 x10^{-6}$

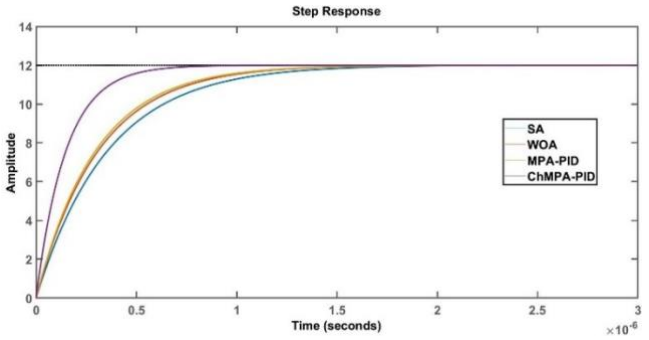

Fig. 17. DC-DC converter step response comparision with different algorithms

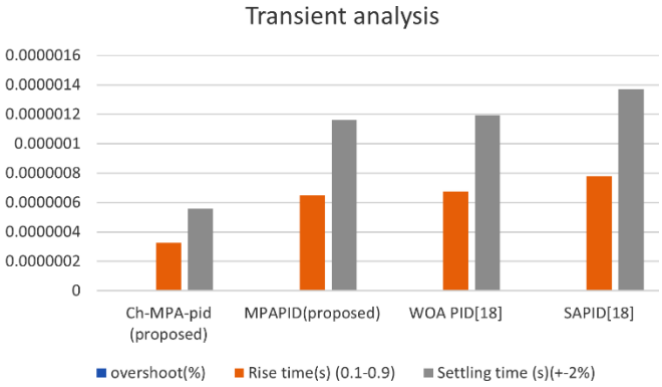

Fig.18. Transient response analysis,bar chart representation

5.3 Frequency Response Analysis

As seen from Fig.19 and table 6 the proposed ChMPA-PID controller is having 180^o phase margin and maximum bandwidth compared to other optimized controllers.

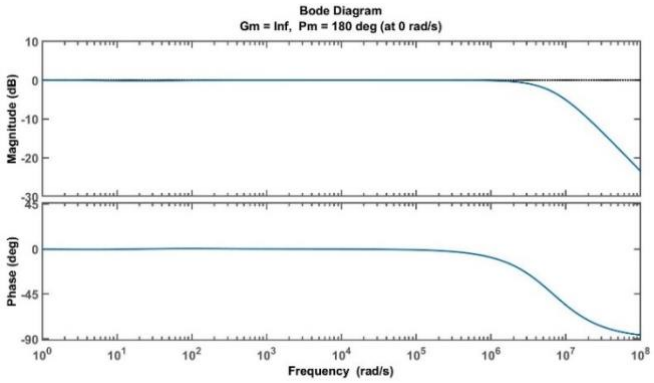

Fig.19. Bode plot of DC-DC converter with ChMPA-PID controller.

Table 6. Bodeplot for Ch-MPA-PID controller

Proposed controllers	Gain margin (db)	Phase margin(c^o)	Bandwidth
Ch MPA PID (proposed)	Infinite	180 °	$6.7141x10^6$
MPA PID (proposed)	Infinite	180 °	$3.3739x10^6$
WOAPID[24]	Infinite	177.1461 °	2.8077×10^6
SA PID[24]	Infinite	177.4675°	3.2334×10^6

5.4 Comparison of Time Domain Integral Error Performance Indices.

The performance time domain integral error indices were compared in table7.Infact ,the ChMPA-PID proposed is effective in transient stability .The bar chart gives the graphical representation of results in Fig.20.The Eqs.(16-19)gives formulas of performance indices ,Tsim=0.00001s.

$$IAE = \int_0^{Tsim} |e|.dt = \int_0^{Tsim} \left|\hat{v}_{ye_f} - \hat{v}_0\right|.dt \quad (16)$$

$$ISE = \int_0^{Tsim} e^2.dt = \int_0^{Tsim} (\hat{v}_{ye_f} - \hat{v}_0)^2.dt \quad (17)$$

$$ITAE = \int_0^{Tsim} t.|e|.dt = \int_0^{Tsim} t.\left|\hat{v}_{ye_f} - \hat{v}_0\right|.dt \quad (18)$$

$$ITSE = \int_0^{Tsim} t.e^2.dt = \int_0^{Tsim} (\hat{v}_{ye_f} - \hat{v}_0)^2.dt \quad (19)$$

Table 7. Values of performance Indices

Proposed controllers	IAE	ISE	ITAE	ITSE
Ch MPA PID (proposed)	1.811 x10^{-6}	0.8547 x10^{-5}	0.4102 x 10^{-12}	0.4216 x 10^{-12}
MPA PID (proposed)	3.593 x10^{-6}	2.125 x10^{-5}	1.3 x10^{-12}	3.141 x 10^{-12}
WOAPID [24]	3.7697 x10^{-6}	2.2216 x10^{-5}	1.6380 x 10^{-12}	3.4267 x 10^{-12}
SA PID[24]	4.3428 x10^{-6}	2.5585 x10^{-5}	2.1246 x 10^{-12}	4.5438 x 10^{-12}

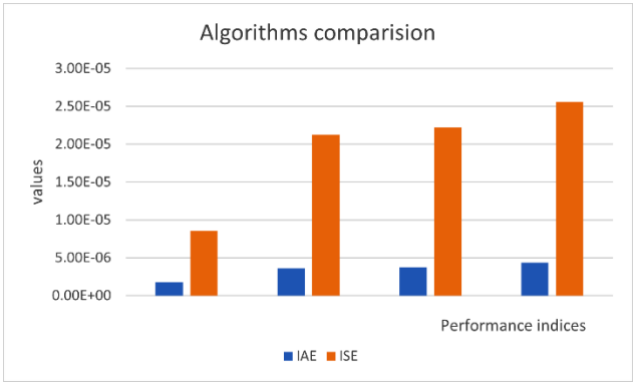

(a)

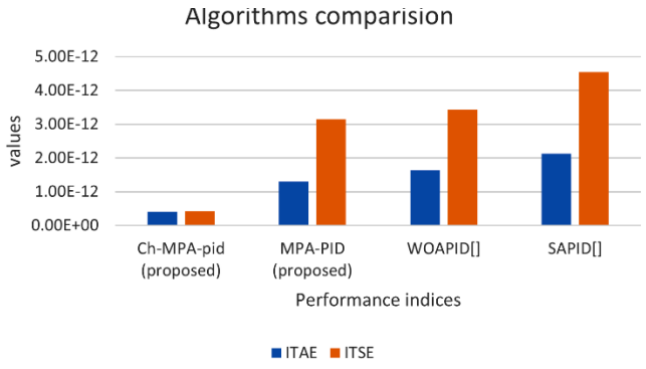

(b)

Fig. 20. Bar chart representation of performance Indices
a)IAE,ISE b)ITAE,ITSE

5.5 Mitigation of Unexpected Disturbance Effects.

At t=3x10^{-6} disturbance is caused ,given a voltage 14V for a short duration and as shown in Fig.21 .The proposed is quicker and best in the disturbance rejection.

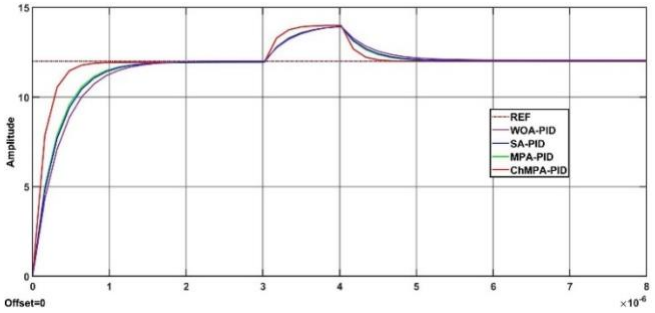

Fig. 21. Mitigation of disturbance.

6 Robustness Analysis

In abnormal cases, the system should maintain an acceptable response ,and when subjected to uncertainties, the robustness analysis was observed .For achieving this, Load resistance (R_L) and input voltage is increased by ±50% and±40% respectively. The tables 9-12 and Fig.22-25 shows the transient response and step response respectively. By observing the proposed ChMPA-PID and MPA-PID showing the least values and robustness analysis have been validated for DC-DC forward buck converter voltage control.

Table.8.Modes of operation

Modes	Vin(volts)	RL (*ohm*)
1	22	3
2	22	9
3	50	3
4	50	9

Table.9.Mode-1 results for transient response

controllers	Rise time (0.1→0.9)	Settling time (s)(±2%)	Over shoot (%)
ChMPA PID	5.3527x10^{-7}	9.5962x10^{-7}	0
MPA PID	1.0671x 10^{-6}	1.925x10^{-6}	0
WOA [24]	1.1077x10^{-6}	1.96x10^{-6}	0
SA [24]	1.2748x10^{-6}	2.2502x10^{-6}	0

Table.10. Mode-2 results for transient response

controllers	Rise time (0.1→0.9)	Settling time (s)(±2%)	Over shoot (%)
chMPA PID	5.3439x10^{-7}	9.5359x10^{-7}	0
MPA PID	1.0636x 10^{-6}	1.95005x 10^{-6}	0
WOA [24]	1.1041x10^{-6}	1.9362x10^{-6}	0.0806
SA [24]	1.27x10^{-6}	2.2193x10^{-6}	0.1268

Table.11.Mode-3 results for transient response.

controllers	Rise time (0.1→0.9)	Settling time (s)(±2%)	Over shoot (%)
chMPAPID	$2.3520\text{x}10^{-7}$	$4.2005\text{x}10^{-7}$	0
MPAPID	$4.6834\text{x}\ 10^{-7}$	$8.38\text{x}10^{-7}$	0
WOA [24]	$4.88\text{x}10^{-7}$	$8.6654\text{x}10^{-7}$	0.0303
SA [24]	$5.619\text{x}10^{-7}$	$9.9665\text{x}10^{-7}$	0.0434

Table.12.Mode-4 results for transient response

controllers	Rise time (0.1→0.9)	Settling time (s)(±2%)	Over shoot (%)
chMPA PID	$2.3503\text{x}10^{-7}$	$4.1888\text{x}10^{-7}$	0
MPA PID	$4.6765\text{x}\ 10^{-7}$	$8.3393\text{x}10^{-7}$	0
WOA [24]	$4.8730\text{x}10^{-7}$	$8.6172\text{x}10^{-7}$	0
SA [24]	$5.6097\text{x}10^{-7}$	$9.9033\text{x}10^{-7}$	0

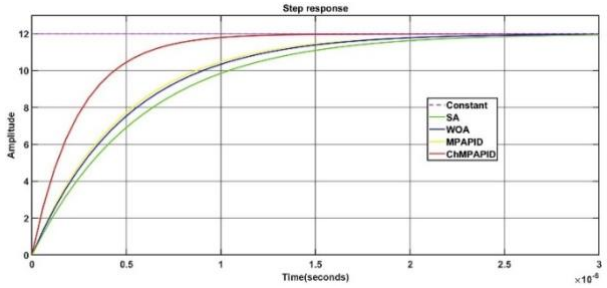

Fig. 22. Mode-1 step response

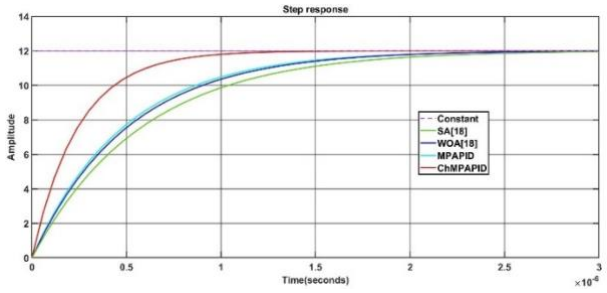

Fig.23.Mode-2 step response

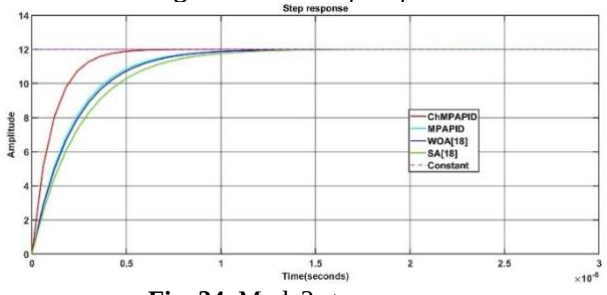

Fig. 24. Mode3 step response

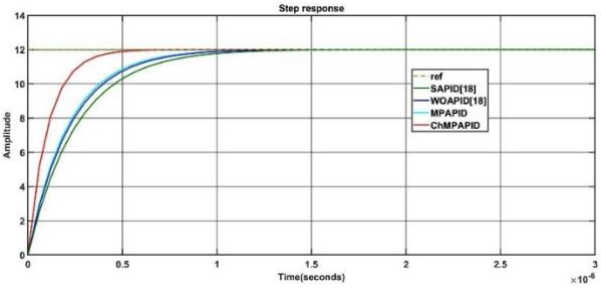

Fig. 25. Mode4 transient response

Fig. 26-29 shows the bar chart comparison of the transient response of four modes

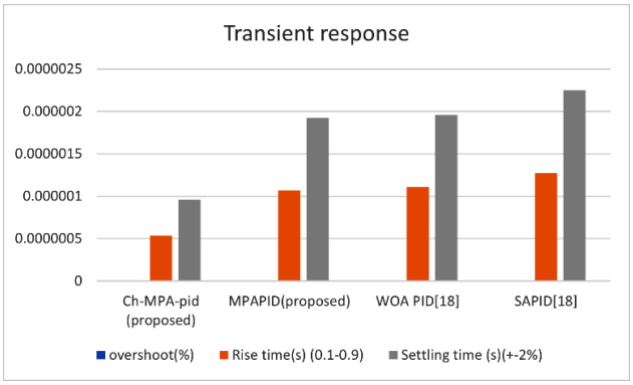

Fig. 26. Mode1-Bar chart depiction

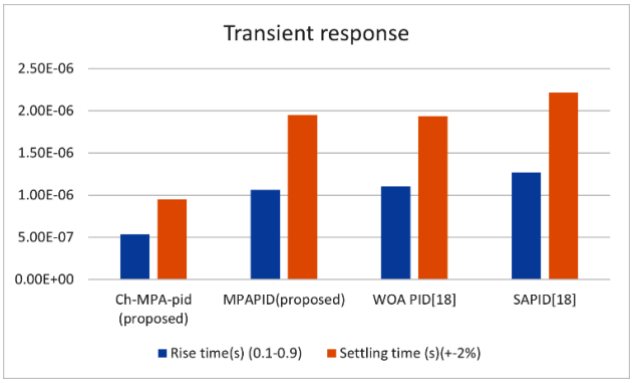

Fig. 27. Mode2-Bar chart depiction

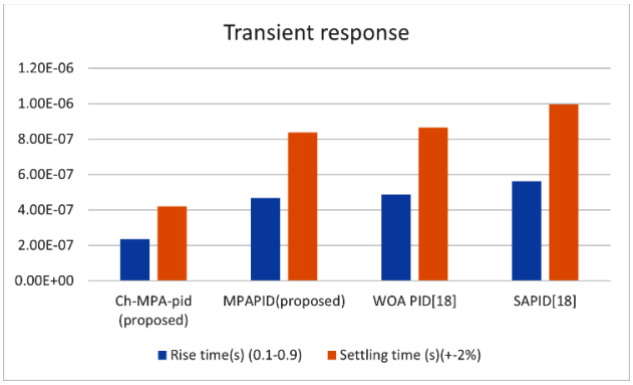

Fig. 28. Mode3-Barchart depiction

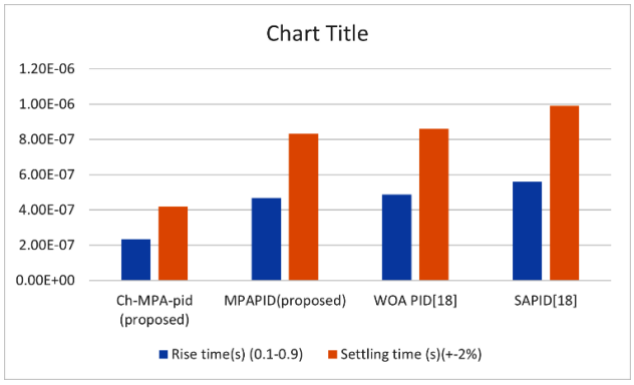

Fig. 29. Mode4-Bar chart depiction.

7 Conclusion

In this article ,firstly a novel design for solid state transformer based pantograph charging electric bus is discussed ,and it provides a 800V dc for battery charging .Then secondly ,dc-dc forward buck converter voltage control is done buy using the novel 'chaotic MPA-PID' controller, which takes ITAE as an objective function ,and is compared with MPAPID ,WOAPID[24] and SAPID[24] in terms of transient ,frequency response and performance indices .Finally ,disturbance rejection scenarios and robustness analysis were done .The proposed charging system is connected to HV side directly and has replaced LFT .The chaotic Marine predators algorithm plus PID controller shown the superior performance in the MATLAB/Simulink platform for a DC-DC forward buck converter system. Limitation is assumed, $V_{in}>V_{ref}$. But in a practical case, when $V_{in}<V_{ref}$,the transformer turns ratio of the forward DC-DC buck converter to increase ,such that the proposed approach will regulate the voltage.

References

[1] X. Liu, " Dynamic response characteristics of fast charging station EVs on interaction of multiple vehicles",IEEE.Access,DOI:10.1109/ACCESS.2020. 2977460, Vol.8, pp. 42404-42421, 2020.(Article)

[2] H. Jing, F. Jia and Z. Liu, "Multi-objective optimal control allocation for an over-actuated electric vehicle",IEEE.Access,DOI:10.1109/ACCESS.2017.2 788941,Vol.6,pp.4824-4833,2018.(Article).

[3] G. Li, Q. Sun, L. Boukhatem, J. Wu. J. Yang, "Intelligent Vehicle to vehicle charging navigation for mobile electric vehicles via VANET-based communication",IEEE.Access,DOI:10.1109/ACCES S.2019.2955927, Vol.7 ,pp .170888-170906 ,2019. (Article)

[4] H. Liang, Z. Lee and G. Li, " A calculation model of charge and discharge capacity of electric vehicle cluster based on trip chain", IEEE Access, DOI: 10.1109/ACCESS.2020.3014160, Vol.8, pp. 142026-142042, 2020. (Article)

[5] S. Liu, D. Xin, L. Yang, J. Li, and L. Wang, " A hierarchical V2G/G2 V energy management system for electric-drive-reconstructed onboard converter ", IEEE Access, DOI:10.1109/ACCESS.2020.3034968, Vol. 8, pp. 198201–198213, 2020.(Article)

[6] D. T. Hoang ,P. Wang, D. Niyato and E. Hossain, "Charging and discharging of plug-in electric vehicles (PEVs) in vehicle-to-grid (V2G) systems: A cyber insurance-based model", IEEE Access, DOI: 10.1109/ACCESS.2017.2649042, Vol.5,pp.732–754, 2017.(Article)

[7] G. Ali, U. Baki Zafer and B. Emine. "Optimal Battery sizing for electric vehicles considering Battery Ageing.", 2022 IEEE 11thInternational conference on Renewable Energy Research and Application (ICRERA),Istanbul, sep, 18-21, 2022, pp.82-89 DOI :10.1109/ICRERA55966.2022.9922669.(conference)

[8] M. Akhil, D. Emrah and R. Ramazan . "A coordinated EV charging scheduling containing PV system", International journal of smart grid, Vol .6, No.3,pp 65-71, 2022.(Article)

[9] H. Jin, N. Sarvar Hussain,L. Sangkeum and H. Dongsoo. "Power Management of Microgrid Integrated with Electric Vehicles in Residential ParkingStation", 2021 IEEE, 10th International conference on renewable energy Research and application (ICRERA), Istanbul, sep. 26-29, 2021 pp.6570,DOI:10.1109/ICRERA52334.2021.9598765. (Conference)

[10] M. Akil,D. Emrah and B.Ramazan. "Analysis of electric vehicle charging demand forecasting model based on Monte Carlo simulation and EMD-BO-LSTM."2022,IEEE,10th International Conference on SmartGrid*(icSmartGrid)*,Istanbul,june,27..29,pp356.. 362,2022,DOI:10.1109/icSmart55722.2022.9848555.(Conference)

[11] O. Hayes. "Discrete-Event Simulation of Electric Transit Buses for Broome County Transportation", 2021, IEEE, 9th International Conference on Smart Grid(icSmartGrid), setubal, june29-01, july, 2021, pp . 27_31,2021,DOI:10.1109/icSmartgrid52357.2021.95 51210. (Conference)

[12] J. W. Kolar and G. Ortiz, "Solid-State-Transformers: Key Components of Future Traction and Smart Grid Systems", in Proc. Of the International Power Electronics Conf. (IPEC), May 2014.(Conference)

[13] J. E. Huber and J. W. Kolar, "Volume/Weight/Cost Comparison of a 1MVA 10 kV/400 V Solid-State against a Conventional Low-Frequency Distribution Transformer," in Proc. of the Energy Conversion Congr. and Expo. (ECCE), pp.4545-4552, sep.2014. (Conference)

[14] A. Q. Huang, M. L. Crow, G. T. Heydt, J. P. Zheng, and S. J. Dale, "The Future Renewable Electric Energy Delivery and Management (FREEDM) System the Energy Internet," 2010 Proc. IEEE, Minneapolis, July

25-29,pp. 133–148, 2010, 10.1109/PES.2010.5589348 (Conference).

[15] M. Steiner and H. Reinold, "Medium Frequency Topology in Railway Applications", in Proc. of the European Conf. Power Electronics and Applications (EPE), Sep. 2007, pp.1-10.(Conference).

[16] C. Wassim, A. Abbou and A. Bouaddi. "Energy Management System for a Stand- Alone Multi-Source Grid Wind / PV/ BESS/ HESS/ Gasturbine/ Electric vehicle Using Genetic Algorithm", International Journal of Renewable Energy Research (IJRER) Vol.13, No. 1 , pp.-202359-69, 2023.(Article)

[17] S. Ekinci, B. Hekimoğlu, S. Kaya, "Tuning of PID controller for AVR system using salp swarm algorithm", in 2018 International Conference on Artificial Intelligence and Data Processing (IDAP), Malatya, Turkey, 2018, pp. 424-429.(Conference)

[18] S. Duman, N. Yörükeren, İ. H. Altaş, "Gravitational search algorithm for determining controller parameters in an automatic voltage regulator system," Turk J Elec Eng & Comp Sci, vol. 24, No. 4, pp. 2387-2400, 2016.(Article)

[19] M. J. Blondin, J. Sanchis, P. Sicard, J. M. Herrero, "New optimal controller tuning method for an AVR system using a simplified Ant Colony Optimization with a new constrained Nelder-Mead algorithm", Appl Soft Comput.,vol.62,pp.216-229,2018.(Article).

[20] A. Jalilvand, H. Vahedi, A. Bayat, "Optimal tuning of the PID controller for a buck converter using bacterial foraging algorithm", in 2010 International Conference on Intelligent and Advanced Systems (ICIAS), Manila, Philippines, 2010, pp.1-5 (Conference)

[21] M. Yaqoob, Z. Jianhua, F. Nawaz, T. Ali, U. Saeed, R. Qaisrani, "Optimization in transient response of DC-DC buck converter using firefly algorithm", in 2014 16th International conference on Harmonics and quality of power (ICHQP), Bucharest ,Romania , 2014, pp. 347-51.(Conference).

[22] O.T. Altinoz, H. Erdem, "Evaluation function comparison of particle swarm optimization for buck converter", in 2010 International Symposium on Power Electronics, Electrical Drives, Automation and Motion,(SPEEDAM),Pisa,Italy,2010,pp.798-802, (Conference).

[23] K.D. Wilkie, M.P. Foster, D.A. Stone, C.M. Bingham, "Hardware-in the-loop tuning of a feedback controller for a buck converter using a GA", in 2008 International Symposium on Power Electronics, Electrical Drives, Automation and Motion (SPEEDAM), Ischia, Italy,2008, pp.680-4. (Conference)

[24] H. Baran, and S. Ekinci." Optimally designed PID controller for a DC-DC buck converter via a hybrid whale optimization algorithm with simulated annealing", Electrica, Vol.20 ,No.1 , pp:19-27, 2020. (Article)

[25] R. Caponetto, L. Fortuna, S. Fazzino, and M. G. Xibilia,"Chaotic sequences to improve the performance of evolutionary algorithms,", IEEE Trans,Evol.Comput.DOI:10.1109/TEVC.2003.810069 , Vol. 7, No. 3, pp. 289–304, June .2003.(Article)

[26] N. S. Jaddi and S. Abdullah, ''Optimization of neural network using kidney-inspired algorithm with control of filtration rate and chaotic map for real-world rainfall forecasting'', Eng. Appl. Artif. Intell., Vol. 67, pp. 246–259, Jan.2018.(Article)

[27] G. I. Sayed, G. Khoriba, and M. H. Haggag, ''A novel chaotic salp swarm algorithm for global optimization and feature selection'', Appl. Intell., Vol. 48, No. 10, pp. 3462-3481, 2018.(Article)

[28] Faramarzi, A., Heidarinejad, M., Mirjalili, S. and Gandomi, A.H., "Marine Predators Algorithm: A nature inspired metaheuristic", Expert systems with applications, Vol .152, pp.1-48, 2020.(Article)

[29] H. Mahammad A., P.J ern Ker, M. S. Hossain Lipu, Z. Hang Choi, M. Safwan Abd Rahman, K. M. Muttaqi and F. Blaabjerg. "State of the art of solid-state transformers:Advanced topologies ,implementation issues ,recent progress and improvements",IEEE Access ,DOI:10.1109/ACCESS.2020.2967345, vol.8 , pp.19113-19132, 2020.(Article)

[30] A .Dipesh, P. Chaturvedi, H. M. Suryawanshi, P. Nachankar, D. Yadeo, and S.Krishna , "Solid state transformer for electric vehicle charging infrastructure", In *2020* IEEE International Conference on Power Electronics, Smart Grid and Renewable Energy (PESGRE2020) , pp. 1-6, 2020, DOI:10.1109/PESGRE45664.2020.9070447 .(Conference)

[31] J. Burkard, and J .Biela, "Hybrid transformers for power quality enhancements in distribution grids-comparison to alternative concepts", In NEIS 2018 Conference on Sustainable Energy Supply and Energy Storagesystems , pp.1-6, september, 2018, VDE.(conference).

[32] https://www.pespublicatiosn.ee.ethz.ch/uploads/tx_ethpublications/workshop_publications/5_10KV-SIC MOSFETs for solid state transformers _ FINAL _ Guillod . pdf, 24th ,may ,2019 .(internet).

[33] G. Ortiz, J. Biela, and J.W. Kolar, "November Optimized design of medium frequency transformers with high isolation requirements", In IECON 2010-36th IEEE Annual Conference on Industrial Electronics Society ,pp.631_638,2010,DOI:10.1109/IECON.2010.5675240. (Conference)

[34] J.E . Huber,and J.W Kolar, "Applicability of solid-state transformers in today's and future distribution grids", IEEE Transactions on Smart Grid, DOI:

10.1109/TSG.2017.2738610, Vol.10, No.1, pp. 317-326, 2017 (Article).

[35] C. Jean-Michel, P. Guerra-Terán, X. Serrano-Guerrero, M. González-Rodríguez, and Guillermo Escrivá-Escrivá. "Electric vehicles for public transportation in power systems : A review of methodologies",Energies ,DOI:10.3390/en12163114, Vol.12, No.16, pp. 1-22, 2019.(Article).

[36] MATLAB, Version 9.70.1190202 (R2023A):The mathworks Inc :Natick,MA,USA,2023.(internet).

[37] N. E .Humphries, N .Queiroz, J. R. M .Dyer, N. G Pade, M. K.Musyl, K. M .Schaefer, D. W .Fuller, J. M . Brunnschweiler, T. K .Doyle, J. D. R .Houghton, G. C .Hays, C.S.Jones, L.R.Noble, V. J Wearmouth, E. J Southall, & D. W. Sims, “Environmental context explains Lévy and Brownian movement patterns of marine predators”, Nature, 465 ,pp .1066-1069, 2010.(Article)

[38] F. Bartumeus, J. Catalan, U. L .Fulco, M. L .Lyra, & G. M .Viswanathan, “Optimizing the encounter rate in biological interactions Lévy versus Brownians trategies” , Physical Review Letters, Vol. 88, No. 9, pp. 097901-1-09790-4, 2002.(Article).

[39] M. Ramezani, B. Danial, and R. Navid. "A new improved model of marine predator algorithm for optimization problems", Arabian Journal for Science and Engineering , DOI : 10.1007/s13369-021-056883, Vol. 46, No. 9 ,pp .8803-8826, 2021. (Article).

[40] J. Too, and A.R Abdullah, “Chaotic atom search optimization for feature selection”, Arabian journal of science and Engineering , DOI:10.1007/s13369-020-044867, Vol.45, No.8, pp. 6063-6079, 2020. (Article)